



## UAS as a Support for Atmospheric Aerosols Research: Case Study

MICHAŁ T. CHILIŃSKI,<sup>1</sup> KRZYSZTOF M. MARKOWICZ,<sup>1</sup> and MAREK KUBICKI<sup>2</sup>

**Abstract**—Small drones (multi-copters) have the potential to deliver valuable data for atmospheric research. They are especially useful for collecting vertical profiles of optical and microphysical properties of atmospheric aerosols. Miniaturization of sensors, such as aethalometers and particle counters, allows for collecting profiles of black carbon concentration, absorption coefficient, and particle size distribution. Vertical variability of single-scattering properties has a significant impact on radiative transfer and Earth's climate, but the base of global measurements is very limited. This results in high uncertainties of climate/radiation models. Vertical range of modern multi-copters is up to 2000 m, which is usually enough to study aerosols up to the top of planetary boundary layer on middle latitudes. In this study, we present the benefits coming from usage of small drones in atmospheric research. The experiment, described as a case study, was conducted at two stations (Swider and Warsaw) in Poland, from October 2014 to March 2015. For over 6 months, photoacoustic extinctionmeters collected data at both stations. This enabled us to compare the stations and to establish ground reference of black carbon concentrations for vertical profiles collected by ceilometer and drone. At Swider station, we used Vaisala CL-31 ceilometer. It delivered vertical profiles of range corrected signal, which were analysed together with profiles acquired by micro-aethalometer AE-51 and Vaisala RS92-SGP radiosonde carried by a hexacopter drone. Near to the surface, black carbon gradient of  $\approx 400$  ( $\mu\text{g}/\text{m}^3$ )/100 m was detected, which was below the ceilometer minimal altitude of detection. This confirmed the usefulness of drones and potential of their support for remote sensing techniques.

**Key words:** Atmospheric aerosols, black carbon, UAS, drone, unmanned aerial vehicle, vertical profiles.

### 1. Introduction

In the last few years, the development of technologies for small unmanned aerial systems (sUAS) made them affordable and easy to use as tools in

research. Elevating small sensors above ground level has significant benefits for atmosphere physics, especially when it comes to aerosol research. Complex interactions between aerosols and solar radiation, together with very limited measurement options of vertical profiles of aerosols' optical and microphysical properties, make understanding and modeling Earth's climate difficult (Bond et al. 2013; IPCC 2013; Koch and Del Genio 2010; Myhre and Samset 2015). Columnar integrated data are available for many properties, but it is important to remember that for some aerosols, such as absorption of black carbon (BC), vertical distribution is even more important than total columnar values (Samset and Myhre 2011; Samset et al. 2013; Zarzycki and Bond 2010; Cook and Highwood 2004). Aerosols play an important role in radiative transfer and Earth's energy budget, both in terms of direct and indirect effects. Recently, we observe an increase of interest in air quality and its influence on human health. Owing to monitoring of large air polluters, local emissions are more strictly controlled. Air-quality monitoring and modeling focus on particle size distribution and their horizontal and vertical variability (Morawska et al. 1999; Vardoulakis et al. 2003; Chan et al. 2005). New ways of acquiring vertical profiles of aerosols near to the ground could significantly improve measurements and, later on, lead to constructing better models and more advanced data processing. Apart from aerosols, drones equipped with proper sensors are able to collect information on trace gases (Brady et al. 2016). Due to their limited endurance, caused by short-lasting electrical power supply, sUAS serve best in experiments where synergy of ground-based soundings and remote sensing data is used. Profiles delivered by tropospheric lidars tend to overlap, and hence, they cannot be used to detect aerosols in the layers close to the surface (Wandinger and Ansmann

<sup>1</sup> Institute of Geophysics, Faculty of Physics, University of Warsaw, Warsaw, Poland. E-mail: mich@igf.fuw.edu.pl

<sup>2</sup> Institute of Geophysics, Polish Academy of Sciences, Warsaw, Poland.

2002), which means that a researcher is forced to use near-field or dual field of view lidars (Lv et al. 2015).

Multi-rotor electric-powered drones perform very well as tools for capturing vertical profiles of quantities that are important for the purpose of atmospheric science. What makes them particularly useful is their vertical take-off and landing, they are also easy to operate, as they are equipped with sophisticated autopilot systems. Moreover, drones do not produce pollution, typical for combustion engines. Before multi-copters became popular, low-altitude vertical profiles of aerosols were often collected with helium-tethered balloons (Ferrero et al. 2014), but their usage is more limited, due to wind and space requirements. The balloons do not need electrical energy for lifting payload and are able to descend/ascend very slowly, reaching high spatial resolutions. On the other hand, drones can collect vertical profiles much faster than any balloon, reaching time resolution of  $\approx 15$  min per profile. It is worth to mention that each individual profile could be acquired without any additional costs apart from the initial cost of an sUAS ( $\approx 3000$  to 13000 USD) and its maintenance parts. This means that this method is very cost-efficient, especially during long field campaigns or measurements in remote locations. Recently many researchers are focused on vertical profiling over remote, fragile locations as Arctic. Many different platforms were used for such measurements as aircraft (Schwarz et al. 2010; Spackman et al. 2010), helicopter (Kupiszewski et al. 2013), or tethered balloon (Ferrero et al. 2016; Markowicz et al. 2017), but there is still need for sUAS dedicated to measurements in Arctic.

The aim of this work is to present the benefits of sUAS usage in atmospheric aerosols research, as proven by the described case study. Our field experiment was conducted in the last quarter of 2014 and first quarter of 2015 in Swider and Warsaw (Poland). The analysed cases contain ground-based measurements with photoacoustic devices, backscatter vertical profiles from ceilometer, and vertical profiles of BC concentration collected by a detector mounted on a detector installed on a drone. Among the presented profiles captured by sUAS, there are a few unique ones, such as severe smog conditions, untraceable by most of lidars.

Thermodynamical profiles acquired together with BC concentration were useful for the analysis of aerosols vertical distribution and relation between temperature inversion and accumulation of aerosols close to the surface.

## 2. Unmanned Aerial Systems in Atmospheric Aerosols Research

Modern science uses many different methods to acquire scientific data related to physics of atmosphere. One of them is data dedicated to optical and microphysical properties of atmospheric aerosols and their interactions with radiation. Most common division of methods discriminate in situ measurement and remote sensing retrieval of quantities as aerosol optical depth (AOD), extinction coefficient, scattering coefficient, absorption coefficient, mass, and particle number concentrations (Hess et al. 1998; Horvath 1993; McMurry 2000; Arnott et al. 2005; Bond et al. 1999; Wiedensohler et al. 2012). In situ measurements are limited spatially, but usually thanks to enough space, power supply and lack of mass limits, they deliver high time-resolution and low-noise results. In case of remote sensing methods, three basic types could be defined: ground-based, aerial, and satellite (Loeb et al. 2007). On ground level, AOD is measured by photometers (Holben et al. 1998), while vertical profiles of extinction/backscattering coefficient or depolarization ratio could be retrieved from tropospheric lidars. Satellites carry radiometers for columnar measurements and lidar for vertical profiles measured from top of atmosphere, down to the ground. Measurements done from an orbit extend to large spaces, covering the whole globe, but with low time-resolution, due to differences in revisit time and changes in cloud cover. During aerial campaigns, both types of measurement could be conducted. Remote sensing and in situ equipment are mounted on aircrafts during dedicated flight-campaigns. This type of campaigns delivers unique data, but incurs significant costs and requires long planning and preparation phase. This makes them episodic, so to speak, and dedicated to special events and basic research rather than monitoring of atmosphere and long-term measurements (Ramanathan et al. 2001; Welton et al.

2002). Small unmanned aerial systems, mostly multi-rotors, could help to fill the gap between in situ and aerial measurements in the aspect of temporal and spatial resolution of atmospheric aerosols measurements. Miniaturized sensors, based on full-scale sensors used in on-ground measurements, could be carried on altitudes up to 2000 m above ground level and deliver vertical profiles of atmospheric aerosol selected properties in the same way as radio-sounding, but in repeatable way, without any need to use new equipment during each flight (Chilinski et al. 2016). Thanks to easy operation technique (professional training takes up to 2 weeks), small size, and almost no cost of a single flight, drones could significantly extend data set of local measurements and improve understanding of lidar vertical profiles together with ground data.

### 2.1. Miniature Sensors

The potential success of small UAS in atmospheric aerosols research lies in miniaturization of sensors, which are light enough to fit in payload limits. Mass is the crucial factor here, and in most cases, 1000–1500 g is the maximum payload; otherwise, it could significantly influence range and flight time. Moreover, ‘flying sensors’ meet the requirements of power efficiency and data storage/transmission. Along with the sensor, a power source must be carried. Some sensors are equipped with internal batteries and convenient when no additional power sources are needed, but usually, it is impossible to change such batteries, so after a flight, the vessel requires downtime for recharging. If we consider using external power supply, depending on drone design, two options are possible. In the first one, the power is supplied by drone’s main batteries, through universal battery elimination circuit (UBEC) with right voltage range. This solution is the best in terms of mass, but could decrease flight time due to additional power consumption, although in comparison with main engines, using up  $\approx 60\text{A}@22.2\text{ V}$  (Chang et al. 2016), consumption of  $\approx 1\text{A}@5\text{ V}$  is minimal. Users do not have to remember about recharging batteries for sensors, but always have access to the main power source. The second option bases on dedicated external battery for powering

payload. It adds some mass to the whole payload, but thanks to small batteries ( $< 100\text{ g}$ , up to 2 h of operation) it is possible to rotate batteries between flight and operate without downtimes, and with no significant reduction of flight time. In real life, all the above ideas are often applied; however, the external payload battery option is probably the most popular.

Apart from supplying power to a sensor, a method for data recording must be secured. There is an approach based on integrated solutions, e.g., internal micro-controller and embedded memory or external data-logger. Another possibility involves devices which transmit data to be stored on-ground, similar to common meteorological radiosondes. External data-logger with a micro-controller is especially efficient when multiple sensors are used during one flight. In such cases, data integration is easier when the entire data stream is saved on one device, with proper timestamps to easily match together all measurements and create unified data output. Sometimes, it is even possible to connect data-logging device to a telemetry channel and send online preview to the ground station. Access to online data is vital for in-flight decision-making: basing on the results, a decision to shorten or extend flight time can be made.

Not disregarding the benefits of miniaturization, such as the aforementioned possibility to mount sensors on small drones, it is important to remember the drawbacks of smaller devices. For example, in situ aerosol equipment with closed measurement chamber which sucks air inside has smaller airflow in their miniaturized versions. Reduced airflow increases noise and causes worse overall performance in signal-to-noise ratio. This requires longer integration times, which in turn decreases spatial resolution of the data. Another factor affecting the results is less-controlled measurement conditions, especially air temperature and humidity. In full-scale devices, air could be dried and heated up to the defined values, whereas in their miniaturized versions, it is impossible, due to limited space and power. It is always important to verify the conditions (ambient or standardized) and parameters that we are measuring. Limitations of small sensors should be checked every time for selected measurement method and measured quantities.

## 2.2. Flight Range/Spatial Resolution

The most common concerns of small UAS users are flight time of the platform and its range of operation. The range depends on flight time, but there is also the second important factor: spatial resolution of data sampling. In vertical profiles, ascent/descent rate and sampling resolution of sensors determine spatial resolution of collected data. Small multi-rotors are usually able to ascend up to 8 m/s and descend up to 4.0 m/s (Pixhawk 2017). Vertical speed and mean flight time determine range, i.e., the maximum altitude of measured profiles. When sensors record data every second, spatial resolution is equal to the vertical speed, but in the case of time-averaging, spatial resolution is decreased. Due to high noise in miniature devices, most of the data need to be smoothed and averaged, and hence, to get better spatial resolutions, drones have to ascend or descend more slowly, which automatically reduces range of profiles. Differences in airflow around a drone during (Luo et al. 2016) ascent and descent require us to carry out multiple flights for different scenarios. To achieve the high spatial resolution and long vertical profile, while maintaining right safety margin, a scenario of fast ascent and slow descent can be chosen. In this scenario, drone ascends with sub-maximal speed until a defined battery level is reached, then it starts to descend slowly onto the ground level (the speed may be increased if the safety level of batteries allows that). To ensure the accuracy of our research, we also prepared a downward profile with higher spatial resolution and smaller airflow around a drone. Table 1 presents estimated vertical

profile range, with different ascent/descent speed for 12-min flight (mean duration of aerosol atmospheric flight for flights in Laboratory of Atmospheric Physics on University of Warsaw).

Crucial stages of interesting aerosol events that are related to anthropogenic emissions take place in the planetary boundary layer, or even lower, at the short distance of a few hundred meters above the surface (Matthias et al. 2004; Nilsson et al. 2001). Consequently, the flight time can be used to improve spatial resolution rather than to collect high profiles. Another approach to this problem benefits from very fast battery changes and almost instant measurement of consequent profiles. Revisit times of around 3–5 min deliver valuable data in the case of very dynamic events. For flights up to 300 m, it is even possible to capture more than one profile on one battery set.

## 2.3. Control and Mission Planning

Most of small UAS are used for ground imaging purposes, so the most common way of controlling them is manual take-off/landing and pre-programmed flight, controlled by autopilot through waypoints defined by the ground control/mission planning software. This approach is the best when the point of interest is well defined spatially and the flight is conducted in stable conditions. For vertical sounding with sUAS, pre-programmed flight patterns can be used for low-altitude flights, when there is a safety margin for battery capacity. For higher flights, over a few hundred meters above the ground, wind conditions may be different than those on the ground due to

Table 1

*Vertical range in meters of sUAS for 12-min flight with different ascend/descent speed*

	Descent (m/s)				
	4.5	4.0	3.0	2.0	1.0
Ascend (m/s)					
6.0	1851	1728	1440	1080	617
5.0	1705	1600	1350	1029	600
4.0	1525	1440	1234	960	576
3.0	1296	1234	1080	864	540
2.0	997	960	864	720	480
1.0	589	576	540	480	360

stronger winds and gusts. In such flights, constant careful observation of battery voltage and drone behaviour is a necessity. Autopilots can terminate pre-programmed mission if battery voltage threshold is reached; however, there are situations when the voltage drops only for a few seconds due to a wind gust. In such a case, autopilot will abort mission and collected profile is significantly shortened.

There is a very useful feature for simple vertical profiles collection, namely the stabilized mode. This mode allows the autopilot only to hold the drone on an altitude/latitude/longitude (based on pressure and GPS), but it is the operator who manually controls speed and flight direction. In stabilized manual flight, the operator and their ground team (typically, a team consists of three people: operator, operator assistant/observer, and payload operator) make decisions about continuing or terminating the flight. When online data from sensors are available, it is even possible to change ascent/descent speed during the flight to focus on the measurements in the most interesting parts of the actual vertical profile.

### 3. Case Study

In the following section, an example of aerosol research with an aid of sUAS is presented. Institute of Geophysics, University of Warsaw, in cooperation with the Institute of Geophysics, Polish Academy of Science Geophysical Observatory at Swider, conducted an atmospheric aerosols experiment during the last quarter of 2014 and the first quarter of 2015. The goal of the experiment was to measure variability of black carbon concentration during the heating season in the center of Warsaw and in one of the surrounding towns. During winter, small towns suffer from high local emissions from household heating systems (Zawadzka et al. 2013). Central parts of Warsaw are heated by the central heating system, and hence, local emissions are mostly connected with transportation (Holnicki et al. 2017).

#### 3.1. Location

Data used for the experiment were collected from various sites around the city of Warsaw (Poland) and

supported by radio-soundings from the third station. An overview map (Fig. 1) presents location of all of those sites. In Warsaw and Swider, in situ measurements with The Photoacoustic Extinctionmeters (PAX) were conducted. In Swider Geophysical Observatory (52.11°N, 21.23°E, 94 m. asl), we had a Vaisala CL31 ceilometer operating and all of the described drone flights were made there. The station in Warsaw (52.21°N, 20.98°E, 112 m. asl) is located 4 km from the largest airport in Poland (Warsaw Chopin Airport  $\approx$  125,000 operations annually) and only 300 m from the Medical University of Warsaw Hospital's helipad. This is the reason why all of the drone operations were done in Swider. In Swider, the controlled traffic region (CTR) is located 600 m above ground level. To ensure safety during the experiment, special air zone was requested, ranging from the ground level up to 1000-m altitude, and 1-km diameter around the Swider station. To verify actual thermodynamical conditions and detect temperature inversion from meteorological soundings, we used the data coming from WMO #12374 Legionowo station (52.40°N, 20.95°E, 73 m. asl).

#### 3.2. Instruments

Photoacoustic Extinctionmeters 870 and 532 nm were used to measure scattering coefficient, absorption coefficient, single-scattering albedo, and BC concentration (Nakayama et al. 2015). The first device was placed in Swider Observatory, 2 m above ground level; the second operated in Warsaw, 18 m above the ground level. Data were integrated for over 60 s and then averaged with running mean and data window of 15 min. BC concentration was calculated with mass absorption cross section  $7.75 \text{ m}^2/\text{g}$  for 532 nm and  $4.74 \text{ m}^2/\text{g}$  for 870 nm. For analysis of BC concentration during low altitude, we used temperature inversion mean values averaged over 15 min from radiosonde start (twice per day, at noon and midnight UTC).

Vertical profiles of backscattering coefficient were collected at Swider station by Vaisala CL-31 ceilometer, which operates at 905 nm (Sokol et al. 2014). Vaisala ceilometers have internal overlap correction done almost to the ground level, which offers one of the best results among widely available



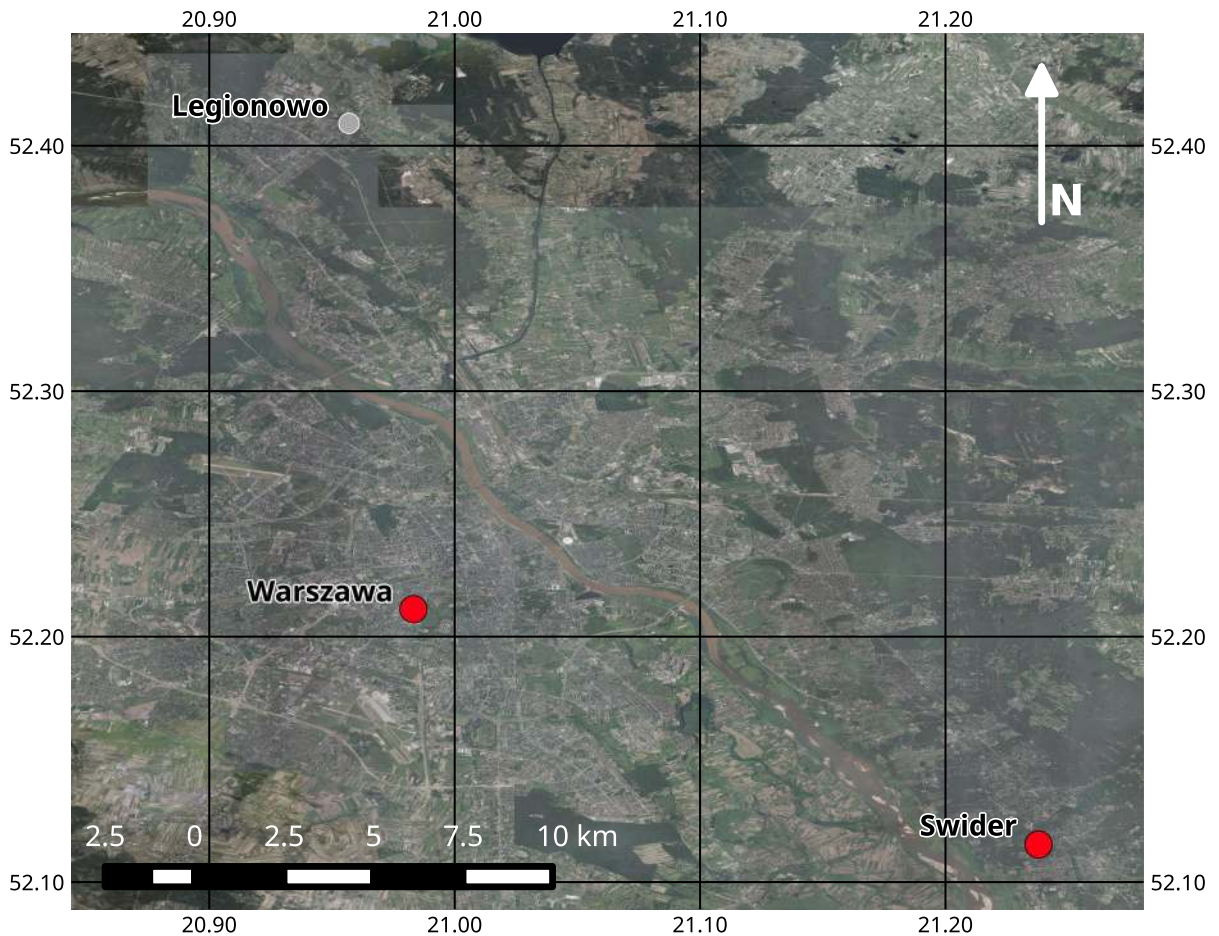


Figure 1

Overview map of measurement stations location (red dots) and WMO station in Legionowo (grey dot)

commercial ceilometers (Madonna et al. 2015). A ceilometer with overlap corrected as low as possible is the best for comparing drone profiles, registered instantly from the ground level. After verification, we assumed that usable profiles were from the range of 60–100 m above ground level. Presented profiles from the ceilometer are the range corrected signal (RCS).

BC concentration measurements were done with a micro-aethalometer AE-51, produced by AethLabs (Ferrero et al. 2014; Chilinski et al. 2016). AE-51 is fully autonomous, which has its own internal battery and memory, capable of operating for over 12 h. Measurements were done at 880 nm, with 1-s integration time and maximum airflow speed of 0.2l/min. Mass attenuation cross section was assumed

for  $12.5 \text{ m}^2/\text{g}$  and mass absorption cross section for  $4.54^2/\text{g}$ . Total weight of the device is  $\approx 280 \text{ g}$ . The radiosonde used for acquiring thermodynamical profiles was well-known Vaisala RS92-SGP (Nash et al. 2010) with replaced original battery and widely used by WMO stations. Alkaline batteries were replaced with a lithium polymer 7.2V rechargeable battery. The battery replacement made the radiosonde lighter, now weighing  $\approx 200 \text{ g}$ .

sUAS utilized during the experiment was Versa X6sci hexacopter, manufactured by Versadrones from Ireland (Chilinski et al. 2016). The platform used six 15.5" propellers, powered by 340 K/V brushless motors with total torque of 6.6 kg. The total mass of the system is 3.5 kg with 490 g of payload and the average flight time of the drone is around 12

min. During the experiment, flights were manually controlled by an operator with live data feed by 2.4-GHz data link (Fig. 2).

#### 4. Results

In this section, we are going to discuss the outcomes of our experiment. Starting from data analysis, we will focus on vertical profiles of BC collected with the sUAS and background results from other instruments. First, we present differences in BC concentration, scattering coefficient, and absorption coefficient between station in Swider and Warsaw. Then, we proceed to the analysis of the influence of temperature vertical profile, especially low-temperature inversion, on BC concentrations. Next, we overview ceilometer performance in measuring aerosol events near to the ground level. Finally, we describe selected vertical profiles of BC concentration measured by sUAS compiled with corresponding profiles from ceilometer and ground results from PAX.

##### 4.1. Ground Measurement Comparison

At both stations, data were collected for over 6 months, during the heating season of 2014/2015. The first step of the analysis was to determine if there are any significant differences between stations in daily mean values of measured by PAX coefficients and BC concentration. Table 2 presents mean values with

95% confidence intervals for both stations. Due to differences in wavelength of the devices in both stations, only BC concentration could be duly compared. For this reason, further analysis presents data results of monthly anomalies. The anomalies were calculated as percentage difference between mean value for the month and mean value for the entire experiment period (Table 2).

Differences between anomalies with 95% confidence intervals are presented on panels a, b, and c of Fig. 3. Panel d presents the absolute values of BC concentration. Our results show satisfactory correspondence between the stations during the experiment. Although measurements were done in the stations 20 km away from each other, situated in different environment (city center vs. suburban area), the behavior of daily mean anomalies follows the same trend. Discrepancies between the stations are almost completely covered by the uncertainty of results. When we compare the absolute values of BC concentration [Fig. 3, panel d shows slightly higher ( $\approx 10\%$ )] values for Warsaw, but this difference is below statistical significance. The preserved pattern of the monthly changes and difference of results between the stations below uncertainty level suggest that during the analysed period, any significant differences were not detected. This lack of discrepancies proves that despite our assumptions about differing emissions in those two places, higher local emission from heating in Swider is balanced by higher traffic pollution in Warsaw.



Figure 2

Hexacopter Versa X6sci with AE-51 micro-aethalometer and Vaisala RS92-SGP radiosonde

Table 2  
*Mean values of coefficient and BC concentration from 10.2014 to 03.2015*

Quantity	Swider (870 nm)	Warsaw (532 nm)
Scattering ( $\text{mM}^{-1}$ )	$91.6 \pm 33.3$	$168.0 \pm 60.7$
Absorption ( $\text{mM}^{-1}$ )	$15.6 \pm 4.6$	$28.2 \pm 6.7$
BC ( $\mu\text{g}/\text{m}^3$ )	$3.3 \pm 0.9$	$3.7 \pm 0.8$

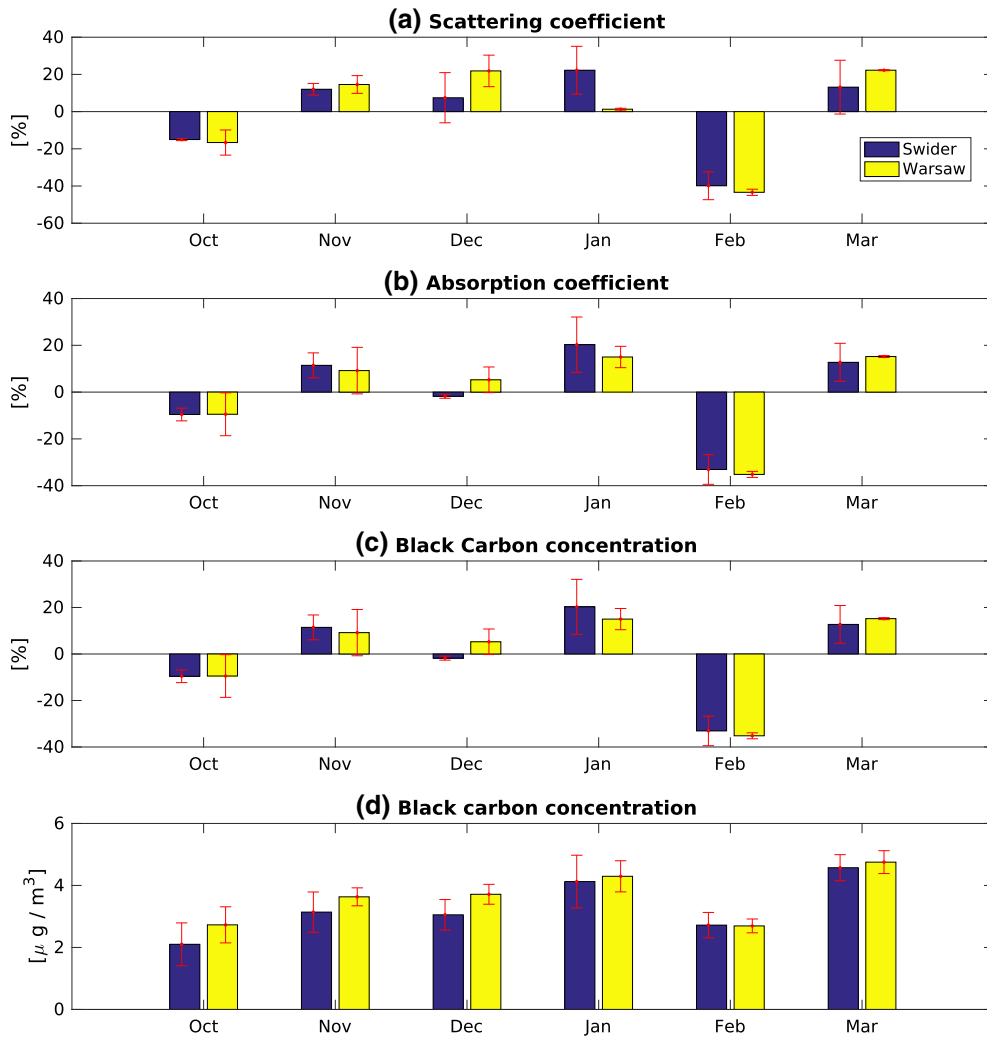


Figure 3

Monthly mean relative anomalies of scattering coefficient (a), absorption coefficient (b), BC concentration (c), and the absolute values of BC concentration (d) at the Swider and Warsaw stations. Blue bars for Swider and yellow for Warsaw. 95% confidence interval marked with red whiskers



#### 4.2. Height of Temperature Inversion and BC Concentration

During the experiment, we examined the relation between smog conditions (days with high BC concentrations) and temperature inversion height. During low-altitude temperature inversion, conditions in the lowest parts of the atmosphere are thermodynamically stable. This prevents air from mixing and accumulates aerosols close to surface. Drones are especially useful for research of aerosols during such conditions when inversion is below its operational range and degree of aerosols accumulation can be investigated. To verify the hypothesis of temperature inversion influence on BC concentration, results from PAX were divided into two classes, basing on the height of temperature inversion. For this analysis, we selected only measurements made at noon and midnight UTC, when radiosonde was launched in the Legionowo station. Data from PAX were averaged for 15 min after radiosonde's launch time. Basing on the results of the radio-soundings, we first distinguished the class of low-altitude temperature inversion for inversion height of 600 m agl; other data points, with higher altitude inversion or no inversion, were categorized into the second class. This data set division is presented on Fig. 4. Mean values in Swider were:  $4.69 \pm 0.74 \mu\text{g}/\text{m}^3$  with inversion below 600 m agl and  $2.28 \pm 0.60 \mu\text{g}/\text{m}^3$  for higher altitude or no inversion. Corresponding results for Warsaw were:  $4.54 \pm 0.47$  and  $2.91 \pm 0.32 \mu\text{g}/\text{m}^3$ . The difference between layers is significant, with almost 1.5–2 times higher BC concentration during days with low-altitude temperature inversion. This result confirms the potential of sUAS for measuring aerosols vertical distribution during smog conditions with low-altitude temperature inversion. Such conditions, where inversion is below operational range of drone, are especially interesting: greater load of aerosols is near the surface, and better signal-to-noise ratio and lower uncertainties make it easier to retrieve data from micro-aethalometers and particle counters (Chilinski et al. 2016).

#### 4.3. Ceilometer and PAX Comparison

At this stage, the issue of detecting smog conditions at the surface during analysis of ceilometer signal was brought up. Due to technological

limitations, tropospheric lidars (represented in our experiment by ceilometer Vaisala CL-31) suffer from insufficiently adjusted overlap, which means that devices are 'blind' to aerosols in the lowest layers of the atmosphere.

The overlap of lidar depending on its design could vary from ten up to hundreds of meters. Atmospheric aerosols scientists can benefit from synergy of lidar and drones profiles, but, on the other hand, drones can fill the gap for results made by overlap limitations. To verify the need for extending lidar measurements on the ground, we compared the differences between the results from the lowest bins of ceilometer with the ground results from PAX (Fig. 5). Simplification of not trivial task of comparing lidar measurements with ground measurements is not an easy task and simplification is necessary (Zieger et al. 2011; Welton et al. 2000). We decided to adopt a simple approach based on anomalies. It is important to mention that PAX measures scattering coefficient of samples in dry conditions in close measurement chamber, while ceilometer registers two-way attenuated backscatter coefficient in ambient conditions. Ceilometer RCS does not contain direct physical meaning; hence, we present only the figure with anomalies. Data from the Swider station were analysed for conditions where relative humidity was below 85%. The anomalies of daily means of scattering coefficient from PAX were compared with the anomalies of daily mean of range corrected signal at 5 lower most bins above overlap from Vaisala ceilometer. During data verification of data from ceilometer, we examined altitude bins between ground and 100-m agl. Detection of aerosols starts at 5th bin, which was around 50 m above the ground level. All bins between 5th and 10th (50–100 m) were examined and all showed the same dynamics, and hence, the average from all 5 bin was selected for the results. The presented figures contain uncertainties on 95% confidence intervals. The results show different level of analogies between measurements from both devices. In December, we have almost the same monthly mean, but in March, the difference is significant: the ceilometer shows strongly negative anomaly, while the PAX slightly positive or almost zero anomaly. In general, in the last quarter of 2014, results are more coherent in terms of value and sign

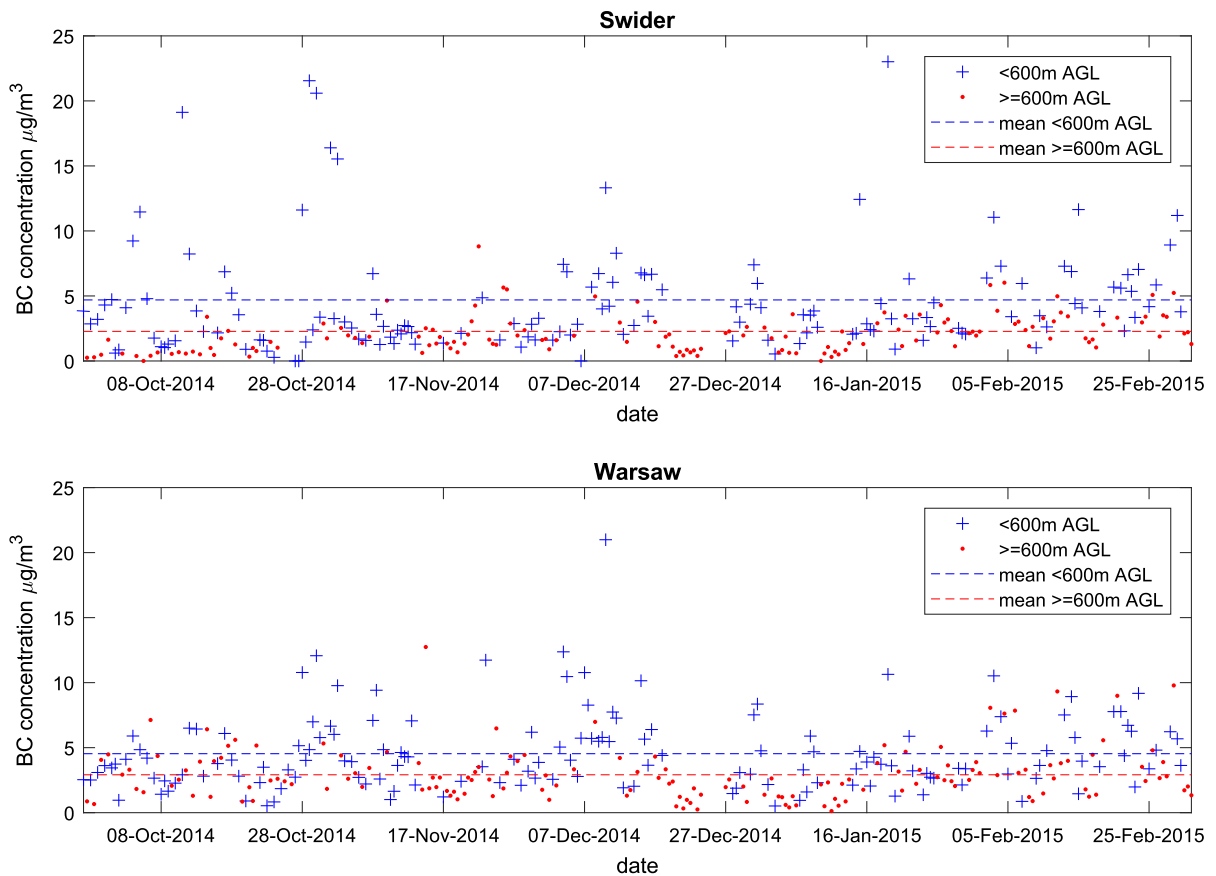


Figure 4

BC concentration in relation to altitude of temperature inversion (Swider on upper panel and Warsaw on lower panel). Blue '+' for measurements when temperature inversion was below 600 m above ground level and red dots for days with temperature inversion above 600 m above ground level. Mean values from all measurements for corresponding groups presented with dashed lines

than in the first quarter of 2015. The reasons for such discrepancies were not thoroughly investigated, but they suggest that there is a vertical variability of atmospheric aerosols distribution even between the lowest levels of Vaisala CL-31 ceilometer and the ground level. This hypothesis ought to be verified by vertical profiles acquired from drones.

#### 4.4. Vertical Profiles of BC Measured by sUAS

During the experiment, vertical profiles of BC concentration with AE-51 aethalometer and RS92-SGP mounted below Versa X6 drone were collected when meteorological and technical conditions allowed. The range corrected signals from Vaisala CL-31 were plotted with BC concentration profiles as

a point for reference and comparison. The profiles from ceilometer are presented only in full overlap region ( $> 60$  m agl). As shown in Sect. 4.2, temperature inversion is an important factor for high aerosols concentrations near to the surface. Thus, each flight was done with a radiosonde and corresponding thermodynamical profiles are presented together with aerosols profiles. In this section, five selected profiles are presented and divided into two flight group sessions: one in the end of October 2014 and the second in February 2015.

The first presented flight session had been conducted for over 24 h between noon of the 28th of October and noon of the 29th of October 2014 (Fig. 6). During those 2 days, a relatively clean air mass was transported from south east of Europe.

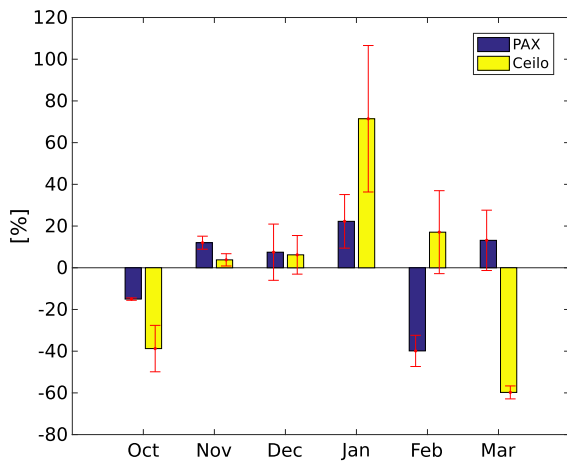


Figure 5

Scattering coefficient monthly mean anomaly from PAX@870 nm (blue bars) in comparison to Vaisala CL-31 lowest bins RCS@905 nm (yellow bars) monthly mean anomaly

AOD measured at the Swider station was only  $0.078@500$  nm and  $0.027@870$  nm with Ångström exponent 1.88. As we saw on RCS, plot boundary layer during that time was at altitudes below 650 m

agl. This gave us a chance to cover all of it during our flights with sUAS. The first flight up to 400 m agl (Fig. 7) was conducted at 11:23 UTC, when BC concentration reported by PAX was below monthly mean ( $2.10 \pm 0.72 \mu\text{g}/\text{m}^3$ ). At that time, the temperature inversion of  $\approx 2^\circ\text{C}$  above 300 m agl was detected. In spite of that, BC profile was quite stable, with regional variations around  $2.5 \mu\text{g}/\text{m}^3$  and potential increase above the flight range in the area of deeper inversion. The ceilometer reported signal near to the background at lowest bins.

The second flight during that session was conducted at night, with very limited altitude, only up to 140 m (Fig. 8). The flight took place during heavy smog conditions, when BC reported by PAX was  $\approx 54 \mu\text{g}/\text{m}^3$ , 25 times the monthly average. Temperature inversion was on the ground level with high-temperature gradient of  $7.2^\circ\text{C}/100$  m. The most interesting here is the profile of BC concentration: rapid decrease from  $\approx 70 \mu\text{g}/\text{m}^3$  at the ground level to  $\approx 4$  at 60 m agl, the change occurring between 40 m and 55 m agl. This resulted in very large local

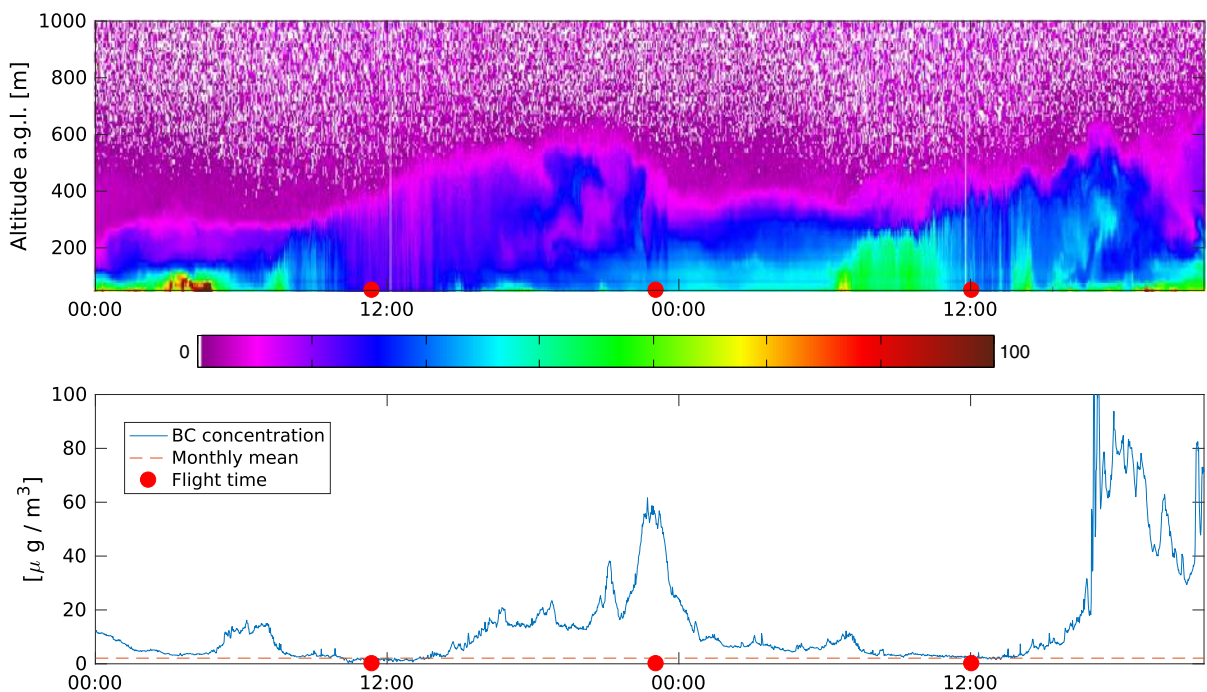


Figure 6

Measurements from 28/29.10.2014 at Swider station. RCS@905 nm from Vaisala CL-31 (upper panel). BC concentrations measured by PAX (lower panel)

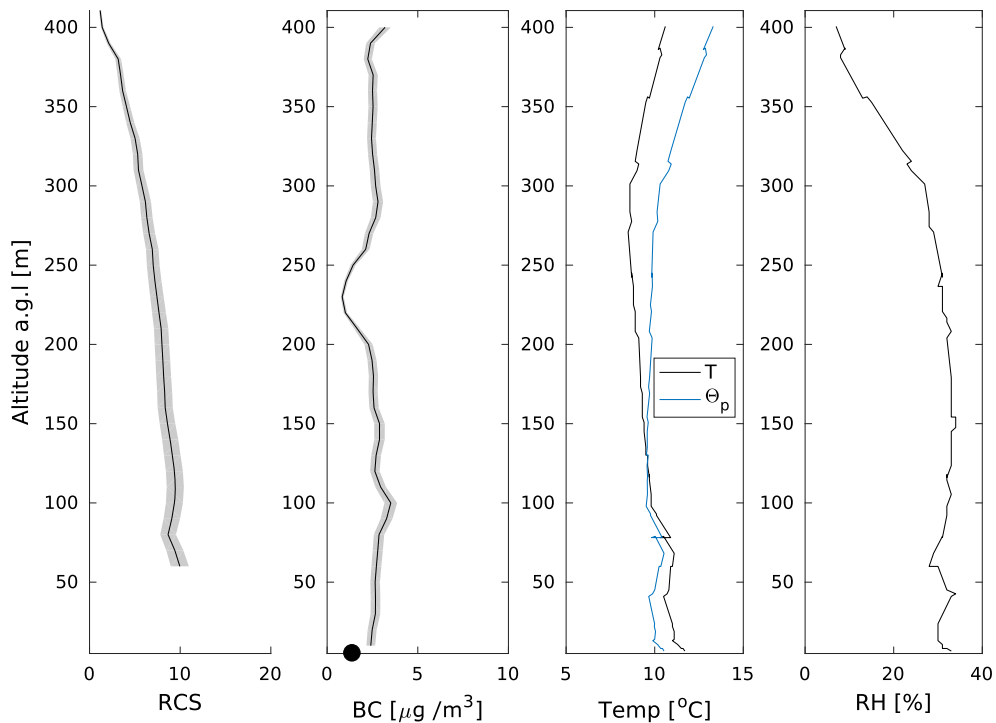


Figure 7

Flight on 28.10.2014 at 11:23 UTC. Vertical profiles of RCS@905 nm from Vaisala-CL31 (RCS), BC concentration from AE-51 (BC), air temperature ( $T$ ), potential temperature ( $\Theta_p$ ) (Temp), and relative humidity (RH). The black dot on BC panel represents BC concentration measured by PAX at the surface

gradient of BC concentration at the level of  $\approx 380 \mu\text{g}/\text{m}^3/100 \text{ m}$ . Figure 9 dedicated to BC concentration profile shows raw BC concentration output reported by AE-51. The concentration was so high that even without any smoothing or averaging, we can clearly see the profile with sharp drop of values at  $\approx 50 \text{ m}$ . What is significant is that almost entire load of BC was below overlap region of the Vaisala ceilometer, which has overlap corrected on a lower level than typical lidars and ceilometers. The signal presented in Fig. 6 at the time of this flight is only slightly higher than the one reported around noon. It confirms that the smog event was almost invisible to the ceilometer.

Last flight from the presented session from October 2014 was made at 12:03 UTC on the following day on 29th of October 2014 (Fig. 10). As on the day before, BC concentration values reported by PAX were close to the monthly mean. AOD on that day was slightly higher:  $0.12@500 \text{ nm}$

and  $0.041@870 \text{ nm}$  with Ångström exponent 1.90. This time, the drone reached 480 m agl and entered zone of temperature inversion above 380 m agl.  $\Theta_p$  shows well-mixed conditions (shallow convection). Both profiles of RCS and BC concentration ( $\approx 2.7 \mu\text{g}/\text{m}^3$ ) were stable to the level of inversion bottom. After reaching 380 m agl, both profiles start to constantly decrease. Correspondence between range corrected signal from ceilometer with BC concentration from aethalometer is easily visible during this flight.

The second flight session took place on the 14th of February 2015 (Fig. 11). The air mass advected from the south of Europe and AOD at the station at the time of the flights was  $0.08@500 \text{ nm}$  and  $0.02@870 \text{ nm}$  with Ångström exponent 1.96. We conducted two flights within the range of 90 min. Monthly mean value of BC concentration based on PAX measurements was  $2.72 \pm 0.82 \mu\text{g}/\text{m}^3$ , but during those flights, the measured values were almost

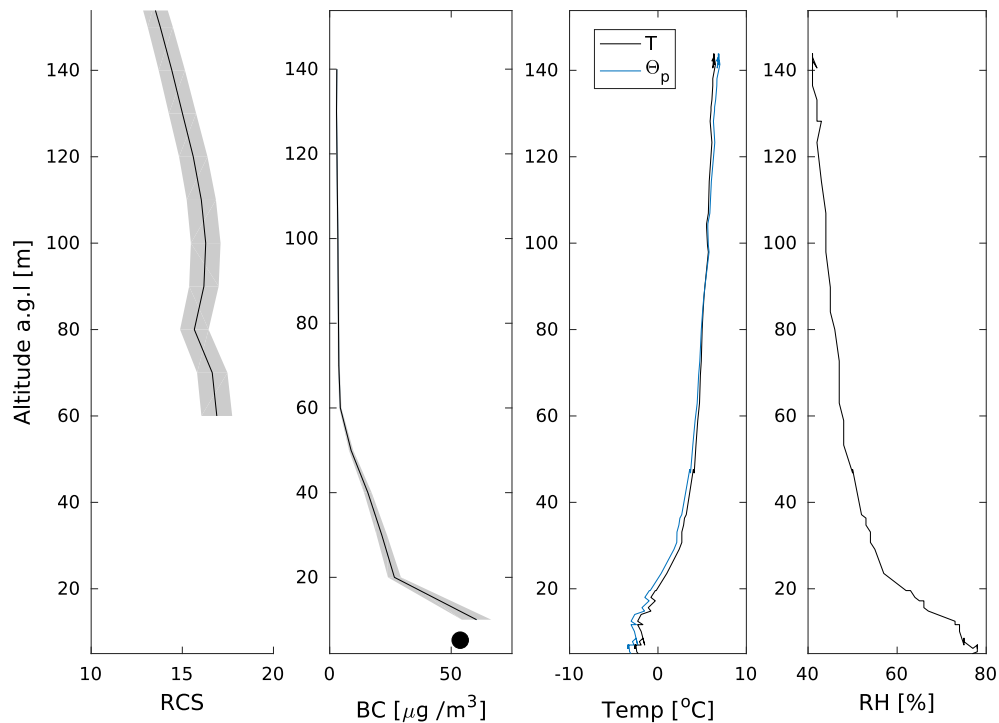


Figure 8  
Flight on 28.10.2014 at 23:04 UTC. Panels description as in Fig. 7

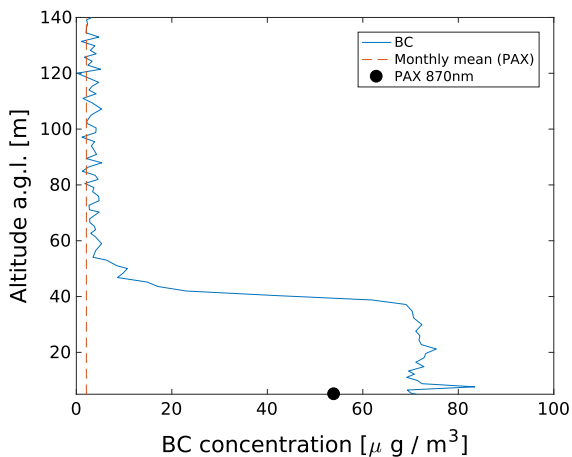


Figure 9  
Flight on 28.10.2014 at 23:04 UTC. Vertical profile of BC concentration measured by AE-51@880 nm with monthly mean and result from PAX at surface

twice as high,  $5.28 \pm 0.42 \mu\text{g}/\text{m}^3$  (hourly mean). The flights (Figs. 12, 13) were done, respectively, at 08:19 UTC and 09:46 UTC. Such consecutive flights show drones' potential for tests with short revisit time and

measurement of dynamic events, such as rising temperature inversion. Elevation of well-mixed air layer extends rising temperature inversion. As in Fig. 12, variability of temperature and relative humidity allows for discerning three layers (0–250, 250–400, > 400 m). The same layers can be observed on the vertical profile of BC concentration and RCS. For the following flight (Fig. 13) shown thermodynamical profiles are simplified, but BC concentration and RCS still follow its pattern. Convection mixing moved the PBL higher, while temperature gradient increased. On 270 m agl, where lower boundary of temperature inversion was located, aerosols started to decrease significantly from  $6.81 \mu\text{g}/\text{m}^3$  at 210 m agl to  $1.62 \mu\text{g}/\text{m}^3$  at 310 m agl (gradient of  $5.19 \mu\text{g}/\text{m}^3/100 \text{ m}$ ). RCS profile followed the trend visible on the BC concentration vertical variability.

The flight session in February 2015 confirmed sUAS capability to measure dynamic changes of aerosol vertical profiles. What is clearly visible in the results is the significant correspondence between thermodynamical profile and profiles of aerosols.



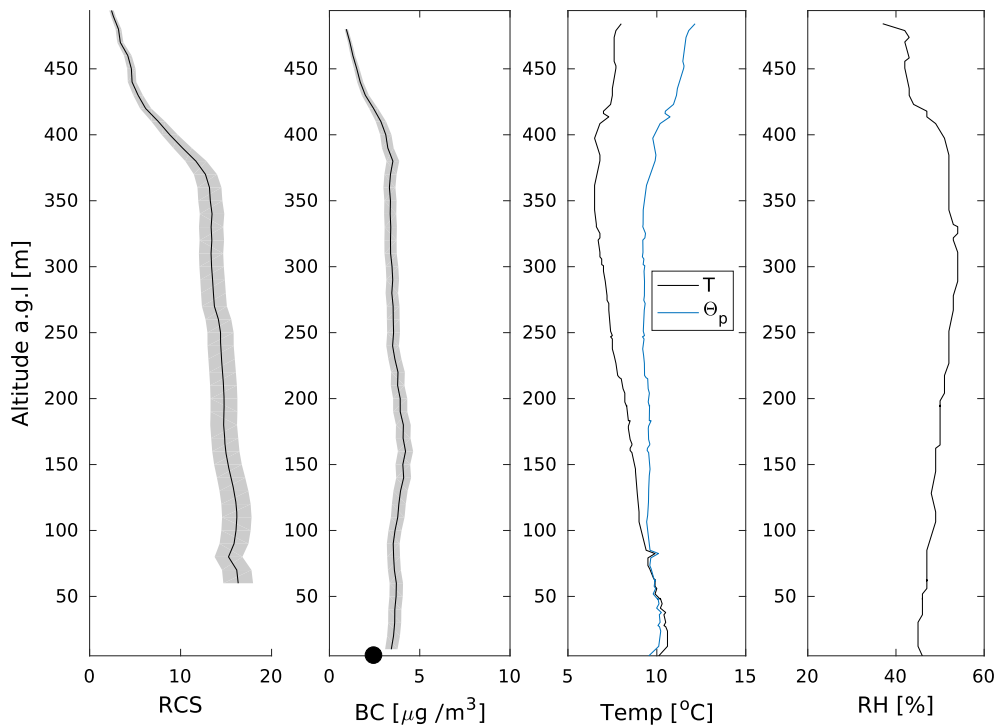


Figure 10  
Flight on 29.10.2014 at 12:03 UTC. Panels description as in Fig. 7

This confirms that measuring aerosol optical properties' profiles should be done together with temperature and humidity profiles. The data obtained from meteorological radiosonde proved to be very useful for better understanding of aerosols vertical variability.

### 5. Summary

Small unmanned aerial systems are very useful for atmospheric aerosols research. First, we introduced the basics of how drones could be applied in atmospheric experiments what benefits they offer for the researchers, as exemplified by our measurement campaign held in Poland (metropolitan area of Warsaw) at the turn of 2014 and 2015. Two field stations were set up for the experiment, one in the center of Warsaw and the second in the suburbs, 20 km away in Swider.

The comparison of black carbon concentration monthly means between the stations did not reveal

any significant differences between them, with the mean value for the entire period of the experiment at the level of  $3.48 \pm 0.91 \mu\text{g}/\text{m}^3$ . Because of different wavelengths on which PAX operated at the two stations, the comparison of scattering and absorption coefficient was based on mean anomaly and, as in the previous case, no significant differences emerged. Verification of the influence of temperature inversion altitude on BC concentration at ground level confirmed our hypothesis that deeper temperature inversion at lower altitudes results in higher BC concentration. On days when temperature inversion was below 600 m agl, mean BC concentration was  $4.61 \pm 0.43 \mu\text{g}/\text{m}^3$ , while on days with no temperature inversion or with inversion on higher altitude, mean value was  $2.60 \pm 0.34 \mu\text{g}/\text{m}^3$ . Due to overlap problems and complex retrieval of lidar data, direct comparison of ground measurements with data from the lowest altitude bins is a difficult issue. Nevertheless, we attempt to do it during the experiment, using Vaisala CL-31 ceilometer, which has relatively well-corrected overlap at  $\approx 50$  m agl. Although

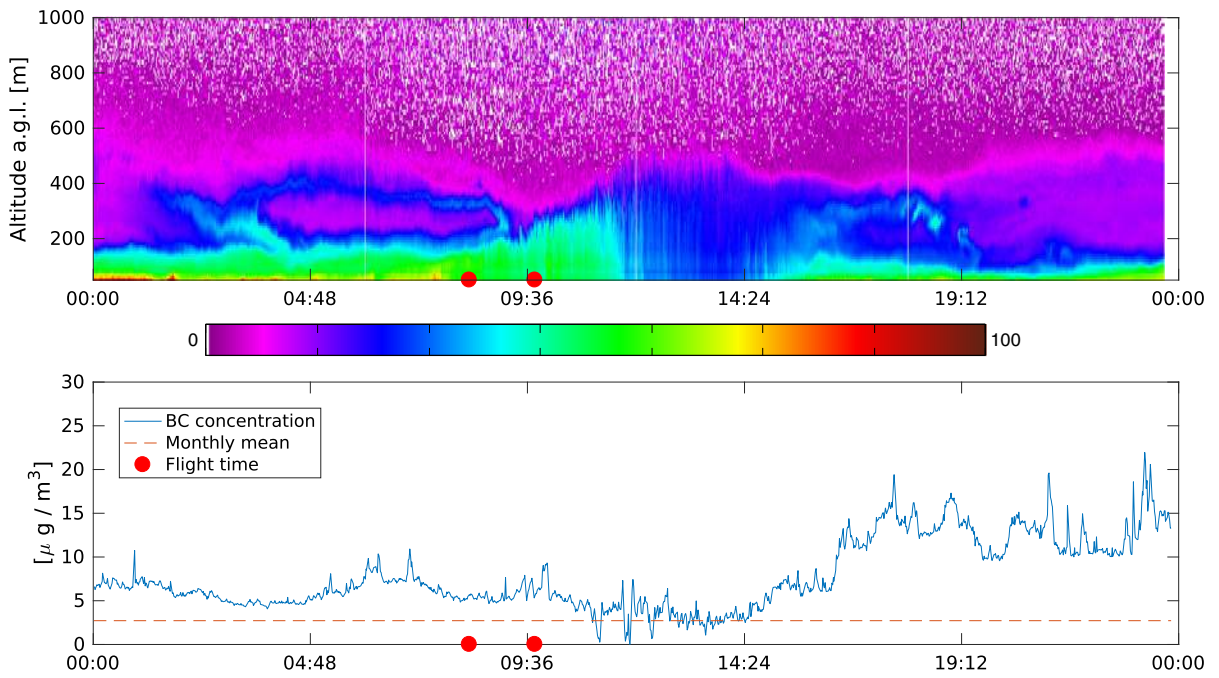


Figure 11

Measurements from 14.02.2015 at Swider. Range corrected signal from Vaisala CL-31 (upper). BC concentrations measured by PAX (lower)

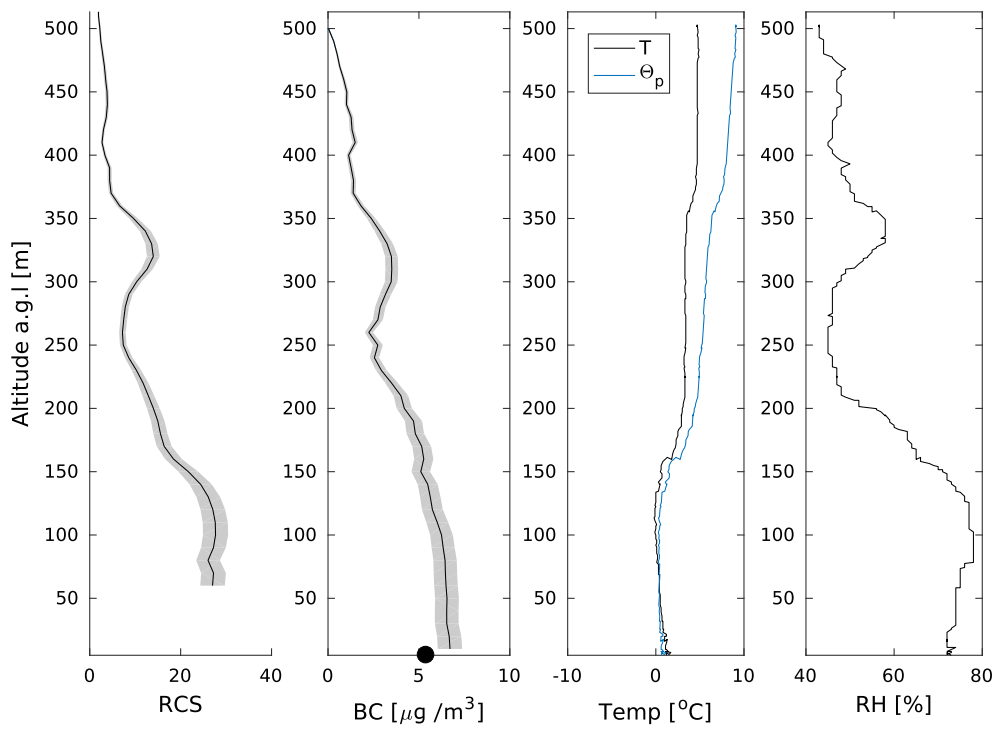


Figure 12

Flight on 14.02.2015 at 08:19 UTC. Panels description as in Fig. 7

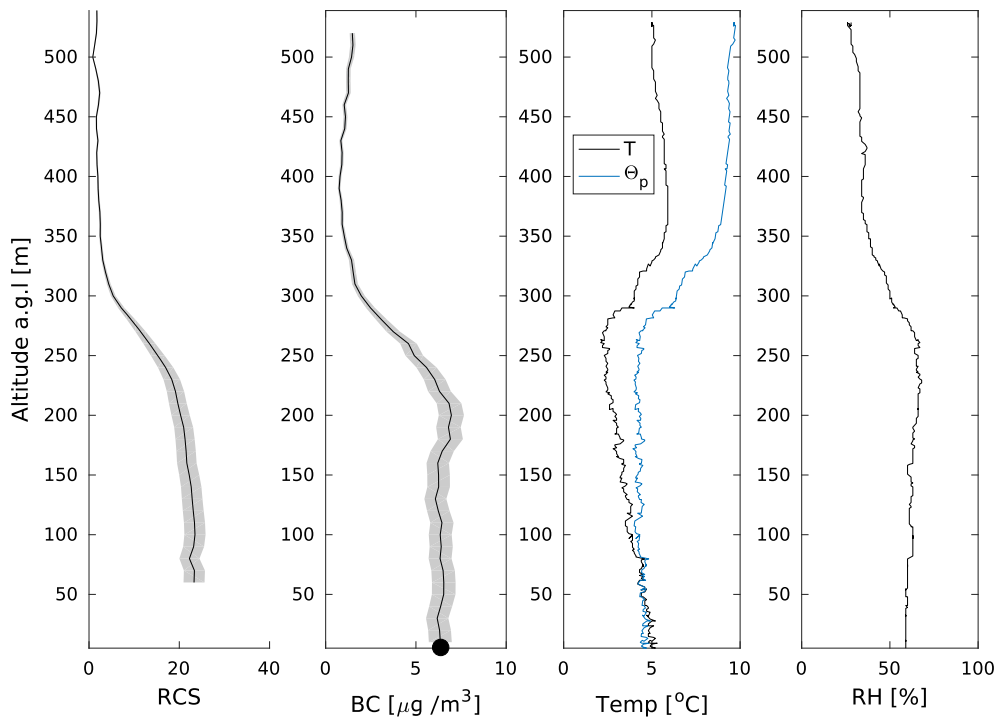


Figure 13  
Flight on 14.02.2015 at 09:46 UTC. Panels description as in Fig. 7

initially promising, the performance of ceilometer in layers directly above the ground level revealed discrepancies with PAX, which are most probably related to the fact that low-altitude aerosol events are not visible on ceilometer.

The results from the two flight sessions with sUAS and the profiles which we collected in the range between 140 and 480 m agl also confirmed good performance of a drone as a support for atmospheric aerosols research. The five profiles presented above give much insight into aerosols vertical distribution near the ground in planetary boundary layer. Drone was able to deliver interesting data of a very strong smog event between the ground level and 60 m above it, with BC concentration gradient of over  $400 \mu\text{g}/\text{m}^3/100 \text{ m}$ . Such events are invisible for most of lidars/ceilometers, what makes drones an exclusive tool for their examination. Drones can also be applied in extending aerosol profiles acquired by lidars: in full overlap region of Vaisala ceilometer, RCS follows vertical variability of BC concentration, and cross-checking both profiles can serve to retrieve

more complex quantities, such as single-scattering properties.

Thermodynamical profiles measured by sUAS reveal dependence of aerosol vertical profile on temperature and humidity variability. Changes in stable layer height, elevation of inversion layer, and variability of humidity have visible influence on aerosol distribution. It supports our idea that measuring vertical profiles of aerosol properties should be checked against basic atmospheric profiles.

Sounding of aerosols with sUAS is a new concept, only recently presented in scientific journals (Chilinski et al. 2016). However, we believe that it has great potential for further development and introduction of new research schemes. Sensors carried by aerial platforms can be technically improved and thus deliver more and more valuable data. Current technological solutions already enable us to install particle counters, spectrometers, radiometers, or sunphotometers on drones. Sufficient potential can be found in solar radiation sensors on horizontal platforms and on sun-trackers, which deliver AOD

profiles, as well as the profiles of heating rate. Moreover, improvement of battery technologies and increase in engines efficiency extend the potential of sUAS, both in terms of operational range and spatial resolution. The popularity of drones is booming and each year a wider variety of models is available on the global market. This offers new opportunities for scientists, and usage of sUAS for research, including atmosphere research, is certainly worth exploring.

### Acknowledgements

This research has been made within the Polish Grant no. 2012/05/E/-ST10/01578 of the National Science Center, coordinated by IGFUW. We acknowledge Brent Holben for preprocessing the AERONET data. CIMEL calibration was performed at the LOA AERONET-EUROPE calibration center, supported by ACTRIS-1 [(European Union Seventh Framework Program (FP7/2007e2013) under Grant agreement no. 262254)].

**Open Access** This article is distributed under the terms of the Creative Commons Attribution 4.0 International License (<http://creativecommons.org/licenses/by/4.0/>), which permits unrestricted use, distribution, and reproduction in any medium, provided you give appropriate credit to the original author(s) and the source, provide a link to the Creative Commons license, and indicate if changes were made.

### REFERENCES

- Arnett, W. P., Hamasha, K., Moosmuller, H., Sheridan, P. J., & Ogren, J. A. (2005). Towards aerosol light-absorption measurements with a 7-wavelength aethalometer: Evaluation with a photoacoustic instrument and 3-wavelength nephelometer. *Aerosol Science and Technology*, 39(1), 17–29.
- Bond, T. C., Anderson, T. L., & Campbell, D. (1999). Calibration and intercomparison of filter-based measurements of visible light absorption by aerosols. *Aerosol Science and Technology*, 30(6), 582–600.
- Bond, T. C., Doherty, S. J., Fahey, D. W., Forster, P. M., Bernsten, T., DeAngelo, B. J., et al. (2013). Bounding the role of black carbon in the climate system: A scientific assessment. *Journal of Geophysical Research-Atmospheres*, 118(11), 5380–5552.
- Brady, J. M., Stokes, M. D., Bonnardel, J., & Bertram, T. H. (2016). Characterization of a quadrotor unmanned aircraft system for aerosol-particle-concentration measurements. *Environmental Science and Technology*, 50(3), 1376–1383.
- Chan, C. Y., Xu, X. D., Li, Y. S., Wong, K. H., Ding, G. A., Chan, L. Y., et al. (2005). Characteristics of vertical profiles and sources of pm<sub>2.5</sub>, pm<sub>10</sub> and carbonaceous species in Beijing. *Atmospheric Environment*, 39(28), 5113–5124.
- Chang, K., Rammos, P., Wilkerson, S. A., Bundy, M., & Gadsden, S. A. (2016). Lipo battery energy studies for improved flight performance of unmanned aerial systems. In *Conference on unmanned systems technology XVIII, volume 9837 of Proceedings of SPIE*, BELLINGHAM. Spie-Int Soc Optical Engineering.
- Chilinski, M. T., Markowicz, K. M., & Markowicz, J. (2016). Observation of vertical variability of black carbon concentration in lower troposphere on campaigns in poland. *Atmospheric Environment*, 137, 155–170.
- Cook, J., & Highwood, E. J. (2004). Climate response to tropospheric absorbing aerosols in an intermediate general-circulation model. *Quarterly Journal of the Royal Meteorological Society*, 130(596), 175–191.
- Ferrero, L., Cappelletti, D., Busetto, M., Mazzola, M., Lupi, A., Lanconelli, C., Becagli, S., Traversi, R., Caiazza, L., Giardi, F., Moroni, B., Crocchianti, S., Fierz, M., Močnik, G., Sangiorgi, G., Perrone, M. G., Maturilli, M., Vitale, V., Udisti, R., & Bolzacchini, E. (2016). Vertical profiles of aerosol and black carbon in the arctic: a seasonal phenomenology along 2 years (2011–2012) of field campaigns. *Atmospheric Chemistry and Physics*, 16(19):12601–12629. <https://www.atmos-chem-phys.net/16/12601/2016/>.
- Ferrero, L., Castelli, M., Ferrini, B. S., Moscatelli, M., Perrone, M. G., Sangiorgi, G., et al. (2014). Impact of black carbon aerosol over italian basin valleys: High-resolution measurements along vertical profiles, radiative forcing and heating rate. *Atmospheric Chemistry and Physics*, 14(18), 9640–9663.
- Hess, M., Koepke, P., & Schult, I. (1998). Optical properties of aerosols and clouds: The software package opac. *Bulletin of the American Meteorological Society*, 79(5), 831–844.
- Holben, B. N., Eck, T. F., Slutsker, I., Tanre, D., Buis, J. P., Setzer, A., et al. (1998). Aeronet—a federated instrument network and data archive for aerosol characterization. *Remote Sensing of Environment*, 66(1), 1–16.
- Holnicki, P., Kałuszek, A., Nahorski, Z., Stankiewicz, K., & Trapp, W. (2017). Air quality modeling for warsaw agglomeration. *Archives of Environmental Protection*, 43(1), 48–64.
- Horvath, H. (1993). Atmospheric light-absorption—a review. *Atmospheric Environment Part A General Topics*, 27(3), 293–317.
- IPCC (2013). *Climate change 2013: The physical science basis. Contribution of Working Group I to the Fifth Assessment Report of the Intergovernmental Panel on Climate Change*. Cambridge University Press, Cambridge. <http://www.climatechange2013.org>.
- Koch, D., & Del Genio, A. D. (2010). Black carbon semi-direct effects on cloud cover: Review and synthesis. *Atmospheric Chemistry and Physics*, 10(16), 7685–7696.
- Kupiszewski, P., Leck, C., Tjernström, M., Sjogren, S., Sedlar, J., Graus, M., Müller, M., Brooks, B., Swietlicki, E., Norris, S., & Hansel, A. (2013). Vertical profiling of aerosol particles and trace gases over the central arctic ocean during summer. *Atmospheric Chemistry and Physics*, 13(24):12405–12431. <https://www.atmos-chem-phys.net/13/12405/2013/>.
- Loeb, N. G., Wielicki, B. A., Su, W. Y., Loukachine, K., Sun, W. B., Wong, T., et al. (2007). Multi-instrument comparison of top-of-atmosphere reflected solar radiation. *Journal of Climate*, 20(3), 575–591.
- Luo, B., Meng, Q. H., Wang, J. Y., & Ma, S. G. (2016). Simulate the aerodynamic olfactory effects of gas-sensitive uavs: A

- numerical model and its parallel implementation. *Advances in Engineering Software*, 102, 123–133.
- Lv, L. H., Zhang, T. S., Liu, C., Dong, Y. S., Chen, Z. Y., Fan, G. Q., Liu, Y., & Liu, W. Q. (2015). Atmospheric aerosols detection research with a dual field of view lidar. *Journal of Spectroscopy*, 2015(2015), 459460. <https://doi.org/10.1155/2015/459460>.
- Madonna, F., Amato, F., Hey, J. V., & Pappalardo, G. (2015). Ceilometer aerosol profiling versus raman lidar in the frame of the interact campaign of actris. *Atmospheric Measurement Techniques*, 8(5), 2207–2223.
- Markowicz, K., Ritter, C., Lisok, J., Makuch, P., Stachlewska, I., Cappelletti, D., Mazzola, M., & Chilinski, M. (2017). Vertical variability of aerosol single-scattering albedo and equivalent black carbon concentration based on in-situ and remote sensing techniques during the iarea campaigns in ny-Ålesund. *Atmospheric Environment*, 164(Supplement C):431–447. <http://www.sciencedirect.com/science/article/pii/S1352231017303953>.
- Matthias, V., Balis, D., Bosenberg, J., Eixmann, R., Iarlori, M., Komguem, L., et al. (2004). Vertical aerosol distribution over europe: Statistical analysis of raman lidar data from 10 European aerosol research lidar network (earlinet) stations. *Journal of Geophysical Research Atmospheres*, 109(D18), 12.
- McMurry, P. H. (2000). A review of atmospheric aerosol measurements. *Atmospheric Environment*, 34(12–14), 1959–1999.
- Morawska, L., Thomas, S., Gilbert, D., Greenaway, C., & Rijnders, E. (1999). A study of the horizontal and vertical profile of sub-micrometer particles in relation to a busy road. *Atmospheric Environment*, 33(8), 1261–1274.
- Myhre, G., & Samset, B. H. (2015). Standard climate models radiation codes underestimate black carbon radiative forcing. *Atmospheric Chemistry and Physics*, 15(5), 2883–2888.
- Nakayama, T., Suzuki, H., Kagamitani, S., Ikeda, Y., Uchiyama, A., & Matsumi, Y. (2015). Characterization of a three wavelength photoacoustic soot spectrometer (pass-3) and a photoacoustic extinctionmeter (pax). *Journal of the Meteorological Society of Japan*, 93(2), 285–308.
- Nash, J., Oakley, T., Voemel, H., & Wei, L. (2010). World meteorological organization instruments and observing methods report no. 107. [http://www.wmo.int/pages/prog/www/IMOP/publications/IOM-107\\_Yangjiang.pdf](http://www.wmo.int/pages/prog/www/IMOP/publications/IOM-107_Yangjiang.pdf).
- Nilsson, E. D., Rannik, U., Kulmala, M., Buzorius, G., & O'Dowd, C. D. (2001). Effects of continental boundary layer evolution, convection, turbulence and entrainment, on aerosol formation. *Tellus Series B Chemical and Physical Meteorology*, 53(4), 441–461.
- Pixhawk (2017). Pixhawk autopilot firmware parameter reference. <https://pixhawk.org/firmware/parameters>.
- Ramanathan, V., Crutzen, P. J., Lelieveld, J., Mitra, A. P., Althausen, D., Anderson, J., et al. (2001). Indian ocean experiment: An integrated analysis of the climate forcing and effects of the great indo-asian haze. *Journal of Geophysical Research Atmospheres*, 106(D22), 28371–28398.
- Samset, B. H., & Myhre, G. (2011). Vertical dependence of black carbon, sulphate and biomass burning aerosol radiative forcing. *Geophysical Research Letters*, 38, 5.
- Samset, B. H., Myhre, G., Schulz, M., Balkanski, Y., Bauer, S., Bernsten, T. K., et al. (2013). Black carbon vertical profiles strongly affect its radiative forcing uncertainty. *Atmospheric Chemistry and Physics*, 13(5), 2423–2434.
- Schwarz, J. P., Spackman, J. R., Gao, R. S., Watts, L. A., Stier, P., Schulz, M., Davis, S. M., Wofsy, S. C., & Fahey, D. W. (2010). Global-scale black carbon profiles observed in the remote atmosphere and compared to models. *Geophysical Research Letters*, 37(18), L18812. <http://dx.doi.org/10.1029/2010GL044372>.
- Sokol, P., Stachlewska, I. S., Ungureanu, I., & Stefan, S. (2014). Evaluation of the boundary layer morning transition using the cl-31 ceilometer signals. *Acta Geophysica*, 62(2), 367–380.
- Spackman, J. R., Gao, R. S., Neff, W. D., Schwarz, J. P., Watts, L. A., Fahey, D. W., Holloway, J. S., Ryerson, T. B., Peischl, J., & Brock, C. A. (2010). Aircraft observations of enhancement and depletion of black carbon mass in the springtime arctic. *Atmospheric Chemistry and Physics*, 10(19):9667–9680. <https://www.atmos-chem-phys.net/10/9667/2010/>.
- Vardoulakis, S., Fisher, B. E. A., Pericleous, K., & Gonzalez-Flesca, N. (2003). Modelling air quality in street canyons: A review. *Atmospheric Environment*, 37(2), 155–182.
- Wandinger, U., & Ansmann, A. (2002). Experimental determination of the lidar overlap profile with raman lidar. *Applied Optics*, 41(3), 511–514.
- Welton, E. J., Voss, K. J., Gordon, H. R., Maring, H., Smirnov, A., Holben, B., et al. (2000). Ground-based lidar measurements of aerosols during ace-2: Instrument description, results, and comparisons with other ground-based and airborne measurements. *Tellus Series B Chemical and Physical Meteorology*, 52(2), 636–651.
- Welton, E. J., Voss, K. J., Quinn, P. K., Flatau, P. J., Markowicz, K., Campbell, J. R., et al. (2002). Measurements of aerosol vertical profiles and optical properties during indoex 1999 using micropulse lidars. *Journal of Geophysical Research Atmospheres*, 107(D19), 22.
- Wiedensohler, A., Birmili, W., Nowak, A., Sonntag, A., Weinhold, K., Merkel, M., et al. (2012). Mobility particle size spectrometers: Harmonization of technical standards and data structure to facilitate high quality long-term observations of atmospheric particle number size distributions. *Atmospheric Measurement Techniques*, 5(3), 657–685.
- Zarzycki, C. M., & Bond, T. C. (2010). How much can the vertical distribution of black carbon affect its global direct radiative forcing? *Geophysical Research Letters*, 37, 6.
- Zawadzka, O., Markowicz, K. M., Pietruczuk, A., Zielinski, T., & Jaroslowski, J. (2013). Impact of urban pollution emitted in warsaw on aerosol properties. *Atmospheric Environment*, 69, 15–28.
- Zieger, P., Weingartner, E., Henzing, J., Moerman, M., de Leeuw, G., Mikkila, J., et al. (2011). Comparison of ambient aerosol extinction coefficients obtained from in-situ, max-doas and lidar measurements at cabauw. *Atmospheric Chemistry and Physics*, 11(6), 2603–2624.